Stochastic forces in circumplanetary dust dynamics

Frank Spahn, Alexander V. Krivov,[1] Miodrag Sremčević, Udo Schwarz, and Jürgen Kurths

Department of Nonlinear Dynamics, Institute of Physics, University of Potsdam, Potsdam, Germany

Received 26 April 2002; revised 18 October 2002; accepted 12 December 2002; published 4 April 2003.

[1] Charged dust grains in circumplanetary environments experience, beyond various deterministic forces, also stochastic perturbations caused, by fluctuations of the magnetic field, the charge of the grains, by chaotic rotation of aspherical grains, etc. Here we investigate the dynamics of a dust population in a circular orbit around a planet which is perturbed by a stochastic planetary magnetic field $\mathbf{B}'$, modeled by an isotropically Gaussian white noise. The resulting perturbation equations give rise to a modified diffusion of the inclinations i and eccentricities e: $\langle \Delta \mathbf{x}^2 \rangle \approx D\,\Delta t$ (here $x = e$ or i, t is time). The diffusion coefficient is found to be $D \propto \omega_G^2\,|\Delta n|/n^2$, where the gyrofrequency, the Kepler frequency, and the synodic frequency are denoted by ω_G, n, and Δn, respectively. This behavior has been checked against numerical simulations. We have chosen dust grains (1μm in radius) ejected from Jupiter's satellite Europa in circular equatorial orbits around Jupiter and integrated numerically their trajectories over their typical lifetimes (100 years). The particles were exposed to a Gaussian fluctuating magnetic field $\mathbf{B}'$ with the same statistical properties as in the analytical treatment. These simulations have confirmed the analytical results. The theoretical studies showed the statistical properties of $\mathbf{B}'$ to be of decisive importance. To estimate them, we analyzed the magnetic field data obtained by the Galileo spacecraft magnetometer at Jupiter and found almost Gaussian fluctuations of about 5% of the mean field and exponentially decaying correlations. This results in a diffusion of orbital inclinations and eccentricities of the dust grains of about ten percent over the lifetime of the particles. For smaller dusty motes or for close-in particles (e.g., in Jovian gossamer rings) stochastics might well dominate the dynamics. *INDEX TERMS:* 6213 Planetology: Solar System Objects: Dust; 6265 Planetology: Solar System Objects: Planetary rings; 2756 Magnetospheric Physics: Planetary magnetospheres (5443, 5737, 6030); 3220 Mathematical Geophysics: Nonlinear dynamics; *KEYWORDS:* rings and dust, nonlinear dynamics, transport processes

Citation: Spahn, F., A. V. Krivov, M. Sremčević, U. Schwarz, and J. Kurths, Stochastic forces in circumplanetary dust dynamics, *J. Geophys. Res.*, *108*(E4), 5021, doi:10.1029/2002JE001925, 2003.

1. Introduction

[2] Dust particles in circumplanetary orbits are subject to numerous forces - gravitational, electromagnetic, radiative, and others. These forces are usually treated in a deterministic way, and their combined action describes fairly well the global characteristics of a dust population [*Burns et al.*, 1984]. This is exemplified by Jupiter's halo [*Horányi and Cravens*, 1996] and gossamer rings [*Burns et al.*, 1999], a tenuous dust ring around the orbits of its Galilean satellites [*Krivov et al.*, 2002], Saturn's dusty E ring [*Horányi et al.*, 1992; *Spahn et al.*, 1999], and many others. However, a more realistic analysis is to take into account that the parameters of the force model may experience sudden, individually unpredictable, and in fact stochastic variations. There are many uncertainties like a possible irregular shape of the dust grains, which influences radiative forces [e.g., *Klačka*, 1994], or charge variations that modify the Lorentz force [*Morfill et al.*, 1980a, 1980b]. Fluctuations of the physical environment (magnetic field, ambient plasma) can further complicate the dust dynamics [*Consolmagno*, 1979, 1980]. Stochastic perturbations in the dust dynamics may markedly alter properties of some of the circumplanetary dust complexes, especially those formed by submicrometer-sized grains and located close to planets, where the stochastic components of the forces are stronger.

[3] In this paper we investigate the influence of a fluctuating contribution to the planetary magnetic field on the dynamics of circumplanetary dust. In other words, in addition to a deterministic magnetic field $\mathbf{B_0}(\mathbf{r})$, a fluctuating part $\mathbf{B}'$ will be considered. Specifically, we will be concerned with the dust environment of Jupiter and therefore will take advantage of the fact that accurate magnetic field measurements by the Galileo spacecraft are available for this planet [*Kivelson et al.*, 1992, 1998]. The question is how do the fluctuations alter the configuration of a dust population? It will be answered by theoretical studies and

[1]On leave from Astronomical Institute, St. Petersburg University, St. Petersburg, Russia.

0148-0227/03/2002JE001925$09.00

will be examined by analyzing the data collected by the magnetometer aboard the Galileo spacecraft in Jupiter's vicinity.

[4] In section 2.1 an analytic diffusion model is constructed by using a Gaussian noise to describe the fluctuating field $\mathbf{B}'$. The outcome of the model is the diffusion coefficients in the space of orbital elements. In section 2.2 the analytic results are checked against numerical simulations. Specific calculations are done for micrometer-sized dust grains ejected from Jupiter's Galilean moon Europa, which have been recently reported to make the largest contribution to a broad tenuous dust ring around the orbits of the Galilean satellites [*Krivov et al.*, 2002]. To check whether, and to what extent, our assumptions about the fluctuating Jovian magnetic field hold true in this region, we analyze the data of the Galileo magnetometer (section 3). Section 4 lists our conclusions.

2. The Model

2.1. Theory of Stochastic Perturbations

[5] The equation of motion of a dust grain in a gravitational and magnetic field of a central body (Jupiter) can be written as

$$\frac{\mathrm{d}^2\mathbf{r}}{\mathrm{d}t^2} = -\nabla\Phi_J + \frac{Q}{c\,m}\left[\frac{\mathrm{d}\mathbf{r}}{\mathrm{d}t}\times\mathbf{B} + \mathbf{E}\right], \tag{1}$$

where $\mathbf{r}$ is the radius vector of a dust grain. For simplicity a point mass potential $\Phi_J = -\mu/r$ has been chosen (where $\mu = GM_J$, G is the gravitational constant, and M_J is the mass of Jupiter). The charge and the mass of the dust grain are denoted by Q and m, respectively, and c is the speed of light. An electrostatic field $\mathbf{E}$ is caused by the magnetic field which corotates with Jupiter:

$$\mathbf{E} = -\mathbf{u}\times\mathbf{B} = -(\boldsymbol{\Omega}_\mathbf{J}\times\mathbf{r})\times\mathbf{B}, \tag{2}$$

where $\mathbf{u} = \boldsymbol{\Omega}_\mathbf{J}\times\mathbf{r}$ is the velocity of $\mathbf{B}$ with respect to an inertial frame (where $\boldsymbol{\Omega}_\mathbf{J}$ is the spin rate of Jupiter).

[6] Furthermore, the magnetic field is assumed to be composed of a deterministic part $\mathbf{B_0}$, and a fluctuating one $\mathbf{B}'$ according to $\mathbf{B} = \mathbf{B_0} + \mathbf{B}'$. In order to simplify the analytical model, we neglect the dipole $\mathbf{B_0}$, and consider only $\mathbf{B}'$, focusing the investigations on the fluctuation-induced diffusion. The particle orbit is described in a coordinate system corotating with the Keplerian angular velocity $\mathbf{n} = \mathbf{e_z}\sqrt{\mu/r^3}$, giving $\mathrm{d}\mathbf{r}/\mathrm{d}t = \dot{\mathbf{r}} + \mathbf{n}(r)\times\mathbf{r}$. The dots denote the derivative with respect to this frame, whereas $\mathrm{d}/\mathrm{d}t$ has to be taken in the inertial frame. In this subsection we will assume initially circular orbits ($\dot{\mathbf{r}} = 0$) for simplicity. We drop both these simplifying assumptions in the numerical calculations (section 2.2), and we shall see that our approach still fully grasps the essential effects of stochasticity.

[7] In the corotating frame the equation of motion (1) becomes

$$\ddot{\mathbf{r}} + 2\mathbf{n}\times\dot{\mathbf{r}} + \mathbf{n}\times(\mathbf{n}\times\mathbf{r}) = -\nabla\Phi_J + \frac{Q}{c\,m}\{[\dot{\mathbf{r}} + (\mathbf{n}-\boldsymbol{\Omega}_\mathbf{J})\times\mathbf{r}]\times\mathbf{B}'\}. \tag{3}$$

The assumptions of initial circularity ($\dot{\mathbf{r}} = 0$), compensation of the central gravity by the centrifugal force rn^2, and motion in the equatorial plane, $\mathbf{r}\times\mathrm{d}\mathbf{r}/\mathrm{d}t = r^2 n(r)\mathbf{e_z}$, reduce equation (3) further

$$\ddot{\mathbf{r}} = \frac{Q}{c\,m}\{[\mathbf{n}\times\mathbf{r}]\times\mathbf{B}'\}. \tag{4}$$

Here, the difference of the rotation rates of the particle radius vector and Jupiter is denoted by $\boldsymbol{\Delta}\mathbf{n} = \mathbf{n} - \boldsymbol{\Omega}_\mathbf{J}$.

[8] For the stochastic part we assume the following properties

$$\mathbf{B}' = \sum_{i=1}^{3} B_i'\,\mathbf{e_i} \tag{5}$$

$$p(B_i') = \frac{1}{\sqrt{2\pi}B_s}\exp\left(-\frac{B_i'^2}{2B_s^2}\right) \tag{6}$$

$$\langle B_i'(t)\rangle = 0, \tag{7}$$

with B_s being the standard deviation of the magnetic field. Two different models are investigated that correspond to different autocorrelations of B_i', uncorrelated fluctuations (equation (8)) and exponentially decaying noise (equation (9))

$$\left\langle B_i'(t)B_j'(t+\tau)\right\rangle = \frac{2\pi}{|\Delta n|}B_s^2\,\delta_{ij}\,\delta(\tau) \tag{8}$$

$$\left\langle B_i'(t)B_j'(t+\tau)\right\rangle = \frac{2\pi}{|\Delta n|}B_s^2\,\delta_{ij}\,\frac{\omega}{2}\exp(-\omega|\tau|) \tag{9}$$

where $\omega = (2\pi)/t_c$ is the cut-off frequency (t_c is the correlation time), $\delta(\tau)$ is Dirac's delta function, and δ_{ij} is the Kronecker symbol. The factor $2\pi/|\Delta n|$ is the normalization time scale which follows from the ergodic theorem.

[9] Instead of solving equation (4), the changes of the osculating orbital elements caused by the fluctuating electromagnetic forces are evaluated. The corresponding Gauss perturbation equations [e.g., *Danby*, 1988] read

$$\dot{a} = \frac{2a^{3/2}}{\sqrt{\mu(1-e^2)}}[(e\sin f)R' + T'(1+e\cos f)] \tag{10}$$

$$\dot{e} = \sqrt{\frac{a(1-e^2)}{\mu}}[R'\sin f + T'(\cos f + \cos E)] \tag{11}$$

$$\dot{\omega} = \frac{1}{e}\sqrt{\frac{a(1-e^2)}{\mu}}\left[-R'\cos f + T'\left(\frac{2+e\cos f}{1+e\cos f}\right)\sin f\right] - \dot{\Omega}\cos i \tag{12}$$

$$\frac{\mathrm{d}i}{\mathrm{d}t} = \sqrt{\frac{a(1-e^2)}{\mu}}\frac{\cos(f+\omega)}{1+e\cos f}\,N' \tag{13}$$

$$\dot{\Omega} = \sqrt{\frac{a(1-e^2)}{\mu}}\frac{N'\sin(f+\omega)}{\sin i(1+e\cos f)}. \tag{14}$$

R', T', and N' are the radial, tangential, and normal components of the fluctuating Lorentz force $\propto (\mathbf{\Delta n} \times \mathbf{r}) \times \mathbf{B}'$ with respect to the Keplerian orbit of the grain $\mathbf{r}(t) = r(t)\ \mathbf{e}_r(t)$.

[10] The Gauss equations (10)–(14) can generally be written in form of a system of Langevin equations

$$\mathrm{d}\mathbf{x} = \hat{\mathbf{A}}(\mathbf{x}) \cdot \mathrm{d}\mathbf{W}'(t), \tag{15}$$

where $\mathbf{x} = (a, e, \omega, i, \Omega)$ is the vector of the orbital elements, $\hat{\mathbf{A}}$ is a coefficient matrix which generally depends on the state vector $\mathbf{x}$, and $\mathrm{d}\mathbf{W}'(t)$ contains terms arising from the stochastic force (R', T', N'). Concerning the concept of stochastic equations and the related stochastic integrals we refer to *Gardiner* [1983] and *Hänggi and Thomas* [1982].

[11] Equation (15) represents a five-component stochastic process, where multiplicative noise $\mathrm{d}\mathbf{W}'$ is assumed to be a Wiener process. Because the stochastic perturbations $\mathrm{d}\mathbf{W}'(t)$ are defined via their statistical properties (e.g., $[\mathrm{d}\mathbf{W}'(t)]^2 = \mathrm{d}t$) [*Gardiner*, 1983] Langevin equations (15) are considered to be solved when the probability density $p(\mathbf{x}, t)$ is found for the case of a definite initial condition: e.g., $p(\mathbf{x}, t_0) \propto \delta(\mathbf{x} - \mathbf{x_0})$. Its evolution is described by the Fokker-Planck equation, which reads for the system (15):

$$\frac{\partial p(\mathbf{x},t)}{\partial t} = \frac{1}{2}\frac{\partial^2}{\partial x_k\, \partial x_l}[D_{kl}(\mathbf{x})\ p(\mathbf{x},t)] \tag{16}$$

$$\hat{\mathbf{D}}(\mathbf{x}) = \hat{\mathbf{A}}^2(\mathbf{x}) = \hat{\mathbf{A}}(\mathbf{x}) \cdot \hat{\mathbf{A}}^{\dagger}(\mathbf{x}). \tag{17}$$

Einstein's sum convention is used in equation (16) with respect to the indices $k, j \in \{1, 5\}$ of the vector of orbital elements $\mathbf{x}$, and $\dagger$ denotes the transpose. For a case when $\hat{\mathbf{D}}$ is independent of $\mathbf{x}$, or in a small time interval $\Delta t = t - t_0$, the solution of equation (16) is a 5-dimensional Gaussian

$$p(\mathbf{x},t) = \left[(2\pi)^5\, \Delta t\, \det\hat{\mathbf{D}}\right]^{-1/2} \times \exp\left[-\frac{1}{2\Delta t}\,(\mathbf{x} - \langle\mathbf{x}\rangle)^{\dagger} \cdot \hat{\mathbf{D}}^{-1} \cdot (\mathbf{x} - \langle\mathbf{x}\rangle)\right]. \tag{18}$$

Here the crucial variable is the diffusion matrix $\hat{\mathbf{D}} \propto \langle(\mathbf{x} - \langle\mathbf{x}\rangle) \circ (\mathbf{x} - \langle\mathbf{x}\rangle)\rangle$ which characterizes the evolution of the system. Its components, the covariances $\langle\mathbf{\Delta x} \circ \mathbf{\Delta x}\rangle \propto (t - t_0)^{\alpha}$, can be derived from Riemann-Stieltjes integration (stochastic integrals) of equation (15). The scaling with time is characterized by the index α. Normal diffusion is found for $\alpha = 1$.

[12] We now apply the treatment sketched above to orbital changes of a swarm of charged grains, which initially form a circle around the central body in the equatorial plane. With the stochastic magnetic field (5)–(7) the components of the related Lorentz force can be written as

$$R' = -N' = \left(\frac{QB'}{mc}\right) r_0\, \Delta n = \left(\frac{QB'}{mc}\right) r_0 n\left(1 - \frac{\Omega_J}{n}\right), \qquad T' = 0. \tag{19}$$

To the zeroth order in eccentricities e and inclinations i, equations (10)–(14) decouple, giving

$$\frac{\mathrm{d}i}{\mathrm{d}t} = \frac{\omega'_G \Delta n}{n} \cdot \cos M + O(e) \tag{20}$$

$$\frac{\mathrm{d}e}{\mathrm{d}t} = \frac{\omega'_G \Delta n}{n} \cdot \sin M + O(e), \tag{21}$$

with the fluctuating gyrofrequency $\omega'_G = QB'/(mc)$ and the mean anomaly $M = n\,(t - t_0)$. The changes of the semimajor axes vanish: $\dot{a} = O(e)$. Variations of ω and Ω are not considered, because they primarily influence the azimuthal structure of the dust configuration, and in this simple consideration we assume axisymmetry.

[13] The reduced system (20)–(21) shows only additive noise, i.e., the state vector $\mathbf{x} = (e, i)$ is absent in the right-hand side of equations (20)–(21), which is advantageous compared to the general stochastic equations (10)–(14) and (15). This means all the problems with the interpretation of stochastic Riemann-Stieltjes integrals do not appear in this simple case, and thus formal integration of equations (20)–(21) leads to

$$\begin{pmatrix} i \\ e \end{pmatrix} = \frac{\Delta n}{n} \int_{t_0}^{t} \mathrm{d}y \begin{pmatrix} \cos M(y) \\ \sin M(y) \end{pmatrix} \omega'_G(y). \tag{22}$$

It should be noted that by taking only the zeroth's order in e and i, we suppress the multiplicative noise. It will become more and more important as the eccentricities and inclinations grow with time. However, as a first estimate of the diffusion coefficients at the beginning of the spreading of the population this assumption seems to be acceptable.

[14] With equation (22) we obtain for the mean square of the eccentricities and inclinations:

$$\left\langle \begin{pmatrix} |i(t)|^2 \\ |e(t)|^2 \end{pmatrix} \right\rangle_{i_0;e_0} = \left(\frac{\Delta n}{n}\right)^2 \times \int_{t_0}^{t}\int_{t_0}^{t} \mathrm{d}y_1\, \mathrm{d}y_2 \cdot \left\langle \begin{pmatrix} \cos M(y_1)\cos M(y_2) \\ \sin M(y_1)\sin M(y_2) \end{pmatrix} \omega'_G(y_1)\omega'_G(y_2) \right\rangle \tag{23}$$

$$= 2\pi\, \frac{|\Delta n|}{n^2}\, \omega_G^2 \times \int_{t_0}^{t}\int_{t_0}^{t} \mathrm{d}y_1\, \mathrm{d}y_2 \cdot \begin{pmatrix} \cos M(y_1)\cos M(y_2) \\ \sin M(y_1)\sin M(y_2) \end{pmatrix} \langle \xi(y_1)\, \xi(y_2)\rangle \tag{24}$$

Here we have denoted by $\omega_G = \omega_G(B_s)$ a gyrofrequency that corresponds to the mean strength of the fluctuating field $B_s = \sqrt{\langle \mathbf{B}'^2 \rangle}$ (see equations (8)–(9)). The autocorrelations are normalized according to $\langle \xi(y_1)\xi(y_2)\rangle = |\Delta n|\langle B'_i(y_1)B'_i(y_2)\rangle/(2\pi B_s^2)$. The indices at the averaging brackets in the left-hand side of equation (23) indicate that the mean has to be taken for an ensemble of dust

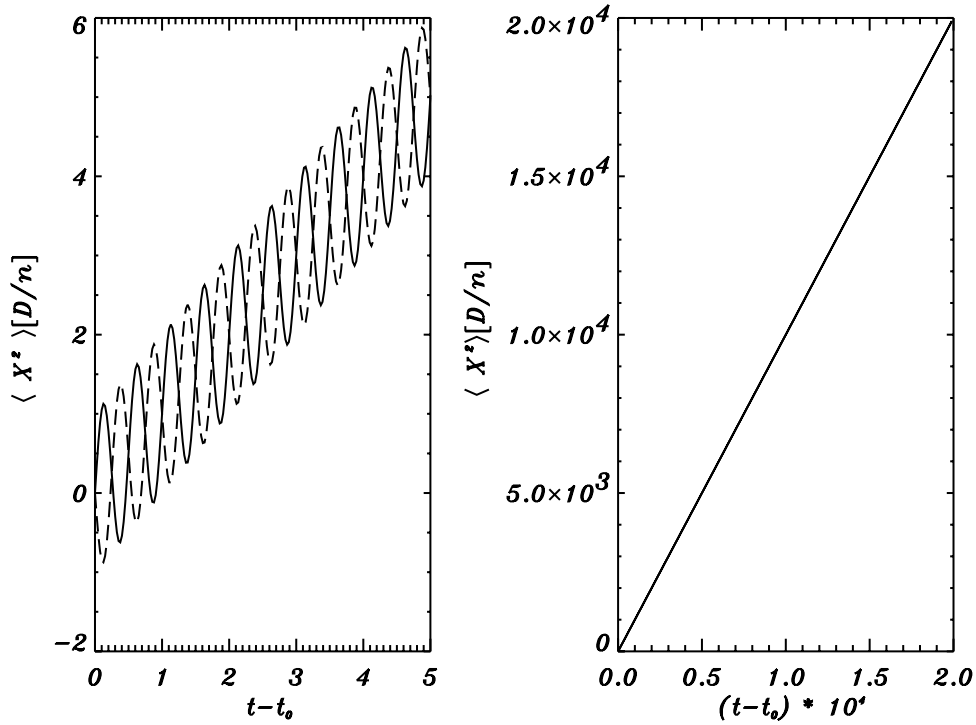

Figure 1. The autocorrelations for eccentricity and inclinations versus time, measured in units of the ratio of the diffusion coefficient over orbital frequency $D/n \approx 10^{-5} \cdots 10^{-6}$. The difference in the diffusive behavior is only recognizable at the very beginning of the diffusion process.

motes having all the initial conditions $e_0 = e(t_0) = 0$ and $i_0 = i(t_0) = 0$.

[15] For both types of the autocorrelation functions (8) and (9) we obtain the following expression for the mean square inclinations or eccentricities:

$$\left\langle \begin{pmatrix} |i(t)|^2 \\ |e(t)|^2 \end{pmatrix} \right\rangle_{i_0/e_0} = D\left[t - t_0 \pm \frac{\sin(2M)}{2n}\right]\left[1 + O\left(\frac{n}{\omega}\right)\right] \quad (25)$$

$$D = \pi \left(\frac{|\Delta n|}{n^2}\right)\omega_G^2(B_s). \quad (26)$$

A normal diffusion ($\alpha = 1$) is modulated with a periodic function. The higher orders of the expansion with respect to n/ω arise from the exponentially decaying noise (9). The results are almost the same for both types of correlations provided that the cut-off frequency is always much larger than the orbital frequency, $\omega \gg n$. The diffusion of the inclinations and eccentricities are shown in Figure 1 indicating that over longer time periods the periodic part in the diffusion becomes increasingly less important. In other words, the simplified model characterizes Gaussian decoupled processes for $p(i)$ and $p(e)$, i.e., the diffusion is a nonstationary Wiener or random walk process.

[16] We restate, however, that the normal diffusion ($\propto t$) will be strongly modified due to the increasing importance of multiplicative noise as soon as the conditions $e, i \ll 1$ are violated.

[17] On the other hand, up to now all estimates have been rather conservative. For instance, provided that all particles of different sizes (r_p is the radius of a spherical grain) acquire one and the same equilibrium electrostatic surface potential [see, e.g., *Horányi*, 1996], the diffusion coefficient depends on size as $D \propto r_p^{-4}$. That means a particle, just half in size, experiences more than an order of magnitude stronger diffusion. In other words, for submicron dust motes stochastic contributions might well dominate the dynamics. However, this also means that the multiplicative noise becomes important quite soon.

2.2. Numerical Experiments

[18] Next, we check our analytical results with the additive noise model with numerical integrations. The main purpose is to find out whether our simplified model of normal diffusion is valid (i.e., whether the predicted square-root spread of particles in the space of orbital elements takes place). Another goal is to estimate when the influence of the multiplicative noise becomes important.

[19] We have considered spherical icy dust grains with radius of 1 μm, charged to +5 V and orbiting Jupiter at a distance of the satellite Europa ($r_0 = a_E \approx 9.5\ R_J$). These grains are believed to make the largest contribution to a tenuous dust ring that encompasses the orbits of the Galilean satellites and has been recently detected *in situ* by the Galileo spacecraft [*Krivov et al.*, 2002]. For these grains, $Q = 1.6 \times 10^{-6}$, $m = 4.2 \times 10^{-12}$ (for the bulk density of 1 g cm^{-3}), $B_0 = 3.4 \times 10^{-3}$ (assuming the strength of 2.95 G at the Jovian equator; see section 3), $c = 3.0 \times 10^{10}$, $n = 2.0 \times 10^{-5}$, $\Omega_J = 1.8 \times 10^{-4}$, $|\Delta n| = 1.6 \times 10^{-4}$ (all values in CGS-ESU units), so that $\omega_G(B_0) = QB_0/(mc) = 4.3 \times 10^{-8}$ and

$$\pi \frac{|\Delta n|}{n^2}\omega_G^2(B_0) = 2.2 \times 10^{-9}. \quad (27)$$

Next, the typical lifetime for such grains around Jupiter, before they are reaccreted by the Galilean satellites or Jupiter, is about 100 years [*Krivov et al.*, 2002]. For this time span, assuming $B_s = 0.05B_0$ (see section 3 for Jovian magnetic field data), equations (25)–(26) predict $D = 5.4 \times 10^{-12}$ sec^{-1}, so that

$$\sqrt{\langle e^2 \rangle} \approx 0.13 \qquad \text{and} \qquad \sqrt{\langle i^2 \rangle} \approx 0.13 \text{ rad} \approx 7.5^\circ. \tag{28}$$

[20] We integrate the equation of motion (1) of a planetocentric dust particle under the point-mass planetary gravity and the stochastic Lorentz force. Integrations are done with the *Everhart* [1974, 1985] routine and a constant integration step Δt. At each step, instantaneous coordinates and velocities of the grain are converted into osculating elements and stored. The deterministic part of the Lorentz force $\mathbf{B}_0$ comes from the aligned corotating dipole magnetic field. The stochastic part is modeled with a white Gaussian noise as follows. Once per integration step, a random $\mathbf{B}'$ vector is added to the deterministic $\mathbf{B}_0$. Namely, B'_x, B'_y, and B'_z are modeled as independent Gaussian deviates with a zero mean and a variance $\sigma = \alpha B_s$, where α is a numerical factor.

[21] This numerical simulation scheme corresponds to the "exact propagator" described by *Mannella and Palleschi* [1989] and *Mannella* [2000], and its accuracy is of the order of the time step: $O(\Delta t)$. The coefficient σ (or α) is found by Taylor expansion of equation (3) and integration of the stochastic part (8) over one time step Δt:

$$\sigma = \frac{1}{\Delta t}\sqrt{\frac{2\pi}{\Delta n} B_s^2 \times \Delta t}. \tag{29}$$

The term under the square root is simply the coefficient in equation (8) times the time elapsed, and the preceding factor $1/\Delta t$ comes into play since we have put the stochastic magnetic field together with the deterministic part into the numerical integration routine. For the numerical simulations, we choose $\Delta t = 500$ sec, so that $\sigma = 8.9B_s$ or $\alpha = 8.9$.

[22] We have made three runs explained immediately below. In each run, one particle was let to go through 100 realizations of the stochastic magnetic field (i.e., a set of individual orbits with the same initial conditions was calculated). As a measure of stochastic effects, we consider, as in the previous section, the orbital eccentricity and inclination, but also computed the evolution of the osculating semimajor axis.

[23] In the first case, we switched off the deterministic dipole magnetic field $\mathbf{B_0}$, exactly as we did in the theoretical model. Since the particles are assumed to have $a = a_E$ and $e = i = 0$ initially, and $a \equiv a_E = \text{const}$, $e \equiv 0$, and $i \equiv 0$ is a solution of the underlying deterministic problem; *all* changes in the three orbital elements come from the stochastic part of the Lorentz force. The results are shown in Figure 2 (left column) and Figure 3 (left panel). The mean spread in e and i does indeed go as the square root of time, as predicted by equation (25). Namely, the best-fit slope to the scatter plots was found to be 0.58 for eccentricity and 0.48 for inclination. The diffusion rate agrees with the rate (28) predicted by the model. Next, there is also a diffusion in the semimajor axis which, however, has different properties. At the beginning of the integration interval, the spread of the semimajor axis is negligible, but it becomes quite pronounced after several tens of years. This can be easily understood; in contrast to equations (20)–(21) for eccentricity and inclination, the equation for a, $da/dt = O(e)$, starts with first-order term in e. Therefore, as soon as appreciable eccentricities are developed, stochastic perturbations in semimajor axis come into play, too. A systematic growth of a indicates a change of the mechanical energy. Obviously, this effect comes from the nonvanishing electric field $\mathbf{E}'$.

[24] In the second case, we restored the deterministic dipole magnetic field $\mathbf{B_0}$ and numerically integrated the full equation of motion (1). The initial conditions were the same as in the previous run: $a = a_E$ and $e = i = 0$. The results are shown in Figure 2 (middle column) and Figure 3 (middle panel). Although they are similar to the previous case, a careful inspection of the plots shows that the diffusion in eccentricity somewhat deviates from the predicted square-root scenario at the beginning of the integration interval (<1 year). A similar effect is seen in the plot of the semimajor axis. These "distortions" become more pronounced for a smaller stochastic force, i.e., for smaller B_s. We have checked that even with $B_s \to 0$, both semimajor axis and eccentricity still exhibit small but nonvanishing oscillations. To explain this, we need to consider the underlying deterministic solution, i.e., that one would have when $\mathbf{B}' = 0$. Interestingly, a circular orbit $a \equiv a_E = \text{const}$, $e \equiv 0$, and $i \equiv 0$ is *not* a solution of the deterministic problem ($\mathbf{B}' = 0$). *Krivov et al.* [2002] have shown that a grain, starting its motion with a circular Keplerian motion, "feels" the reduced inward acceleration of a planet with effective mass $M' \equiv M(1 - L)$, where the L is the Lorentz parameter,

$$L = \omega_G(B_0)\frac{R_J^3 \Omega_J}{GM_J}. \tag{30}$$

Numerically, $L = 0.02$ for 1μm Europa grains considered here. The resulting orbit of a grain will still have $i = 0$, but the semimajor axis and especially eccentricity will oscillate. The amplitude of the semimajor axis oscillations is $\approx 0.0016 a_E$, that of the eccentricity oscillations $- \sim 2L \approx 0.04$. The latter effect explains tangible deviations of the diffusion in eccentricity from the fitting line visible in Figure 3 (middle), especially at $t \lesssim 10$ years.

[25] *Krivov et al.* [2002] suggested the use of modified osculating elements a' and e' that assume the reduced central mass M' and hence differ from the usual osculating elements a and e that refer to a central mass M. The modified elements a' and e' describe the exact Keplerian ellipse followed by a particle influenced by both gravity and the electric part of the electromagnetic force. Note that this ellipse precesses, owing to the magnetic part of the Lorentz force. The third run of our numerical simulation code takes advantage of using these modified, primed elements. Now, we assume the grains to have $a' = a_E$ and $e' = 0$ (and $i = 0$) initially and plot instantaneous values of the modified, rather than usual, osculating elements a' and e'. Interestingly, an orbit $a' \equiv a_E = \text{const}$, $e' \equiv 0$, and $i \equiv 0$ is a solution of the deterministic problem. Therefore *all* deviations of $a' - a_E$, e', and i from zero come from the stochastic part of the Lorentz force. The results, shown in Figure 2 (right column) and Figure 3 (right panel), are very close to the ones depicted in the left column of the same figure which, in

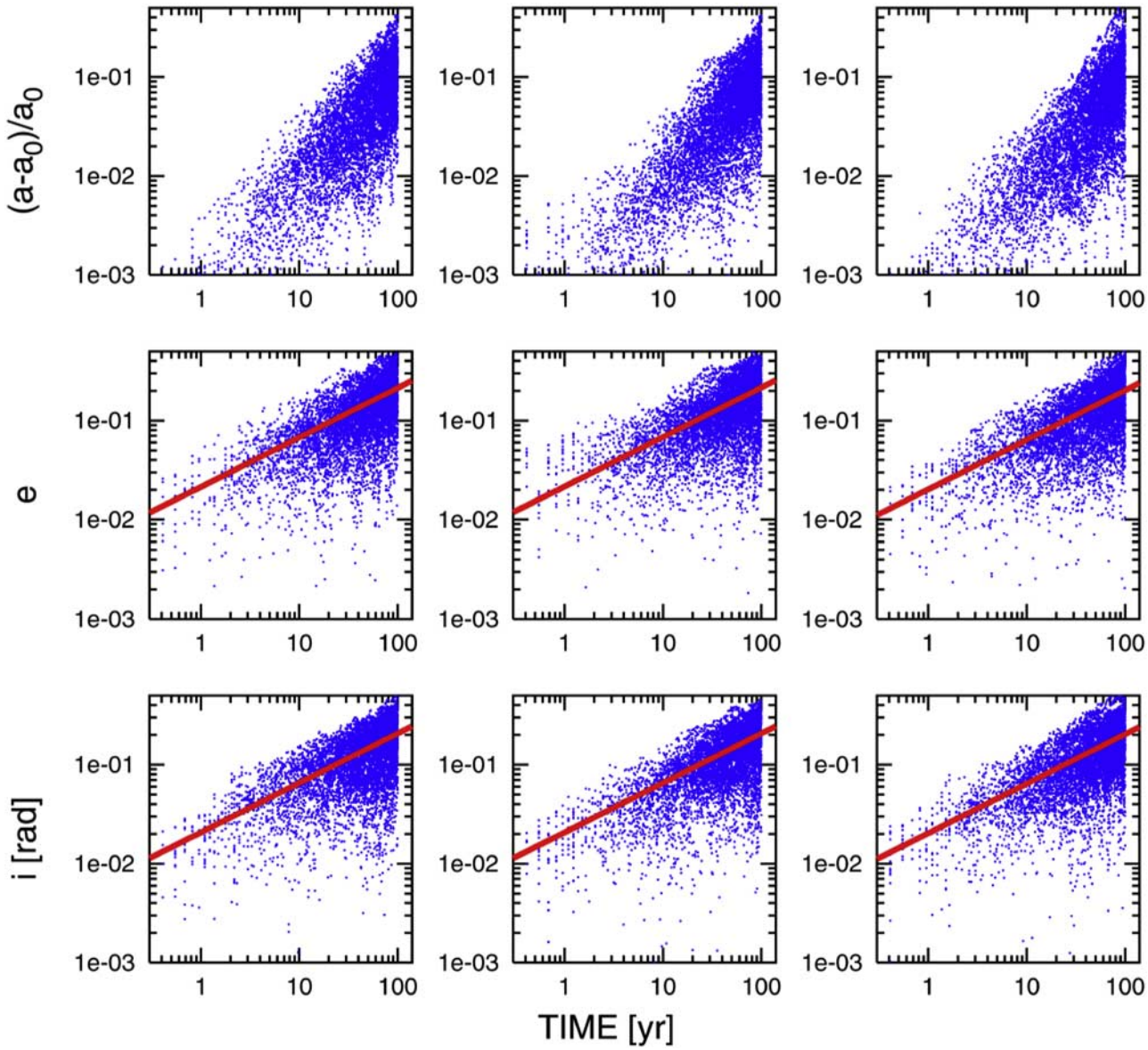

Figure 2. Numerically simulated stochastic effects in semimajor axis (top), orbital eccentricity (middle), and inclination (bottom) of dust grains. Left column: the deterministic dipole magnetic field is switched off. Middle column: dipole is included. Right column: the same as the middle column, but in terms of modified osculating elements. Dots represent instantaneous elements of grains modeled. Lines represent regression fits to the data points, see text for details.

turn, are close to the predictions of the analytic model. In particular, the diffusion in eccentricity no longer deviates from the expected normal diffusion as seen for smaller values of time in the middle figure. The best-fit slope to the scatter plots was found to be 0.56 for eccentricity and 0.53 for inclination.

[26] With additional runs, in which larger strengths of the stochastic field $\mathbf{B}'$ were assumed (not shown in the figure), we checked that the diffusion in $\sqrt{\langle i^2 \rangle}$ and $\sqrt{\langle e^2 \rangle}$ holds linear, as long as i and e are moderate. For $i \sim e \sim 0.3$, deviations from the linear diffusion start to become visible. This is an effect of nonlinear terms (and multiplicative noise) discarded in our analytic model.

[27] Although throughout this paper initially circular, uninclined orbits of particles are considered, we expect that both the qualitative and quantitative conclusions hold true for non-zero, still moderate, initial i and e. This is to say that even in this case equations (25)–(26) give a good idea of the stochastic perturbations in these orbital elements. This conclusion has also been checked and confirmed by numerical simulations.

3. Analysis of the Galileo Magnetometer Data

[28] Finally, we check the assumptions about the statistical properties of noise, used in the above theoretical study, by analyzing the magnetometer data of the Galileo spacecraft [*Kivelson et al.*, 1992, 1998]. The data set has been collected during the last half decade during the orbital tour of Galileo in the Jovian system.

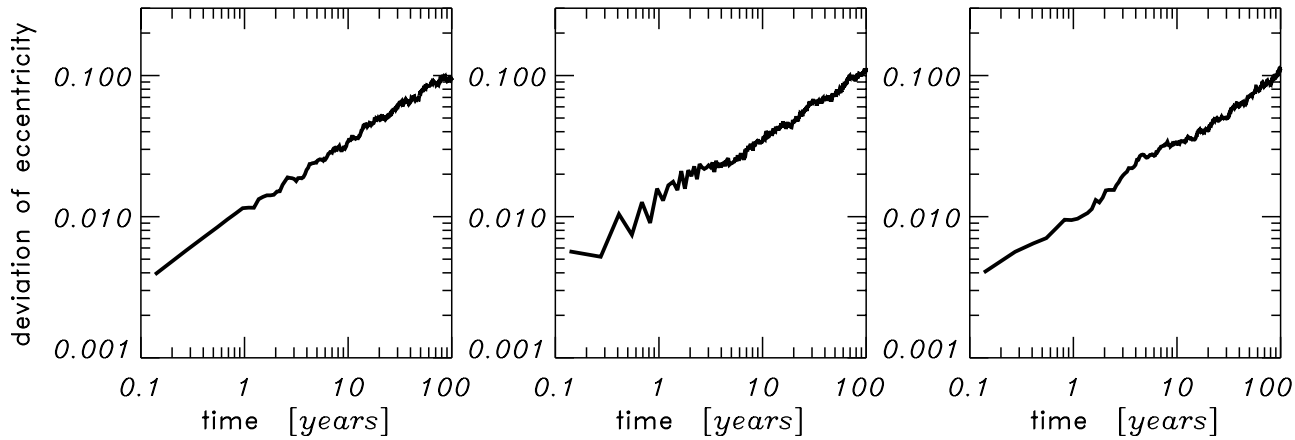

Figure 3. The variances of the eccentricities $\langle\langle e^2\rangle\rangle = \langle(e - \langle e\rangle)^2\rangle$ as a function of time. (left) Without the dipole; (middle) with the dipole and usual orbital elements; (right) same as in the middle column but with modified elements. The effect of taking into the account modified osculating elements is very pronounced for small eccentricities (compare middle and right panels). The left and the right curve are almost the same and show a slope of ≈1/2. These facts demonstrate the validity of the results presented in section 2.1.

[29] The main goal is to characterize the statistical properties of the fluctuating part of the magnetic field $\mathbf{B}'$. This part can be obtained by subtracting the mean field $\mathbf{B}_0$ from the measured field $\mathbf{B}$. To this aim, we have analyzed the magnetic field components $B_r(\mathbf{r}_j)$, $B_\Theta(\mathbf{r}_j)$ and $B\Phi(\mathbf{r}_j)$ (in a jovicentric equatorial spherical coordinate system) measured by Galileo. Index j numerates the orbit of the spacecraft in the region close to Jupiter (i.e., region close to the perijove of Galileo). The spatial resolution of the data is about 500 km (sampling time is 24 sec, $v_{\text{Galileo}} \approx 20$ km/sec). The noise level of the magnetometer was 2 to 3 orders of magnitude less than the data level, depending on the sampling rate and range of the magnetic field *Kivelson et al.* [1992]. The analyzed data were collected along six spacecraft trajectories ($j = 1, 6$) starting on 14 September 1997 (C10), 2 November 1997 (E11), 15 December 1997 (E12), 28 March 1998 (E14), 2 May 1999 (C20), and 19 May 2000 (G28). The perijoves of all these orbits were between the orbits of Io and Europa. Figure 4 shows the measured magnetic field strength as a function of distance from Jupiter.

[30] The magnetic field along the orbits can be decomposed into a time independent main component $\mathbf{B}_0(\mathbf{r})$ and the fluctuating component $\mathbf{B}'(\mathbf{r}, t)$. In the inner region, roughly within Ganymede's orbit (about 15 R_J), and close to the equatorial plane, the time-independent main component $\mathbf{B}_0(\mathbf{r})$ can be well represented with a dipole $B_{\Theta 0}(r)\,\mathbf{e}_\Theta$. We found the relation $|\mathbf{B}_0(\mathbf{r})| \approx \langle \mathbf{B}_{\Theta 0}(\mathbf{r}_j)\rangle_{j=1,6;r_j<27R_J} \propto r^{-3}$ shown in Figure 4 with the dashed line. The slope changes farther out from Jupiter. The solid line in the same figure depicts the best fit for that region.

[31] Keeping in mind that the dipole components at two successive points along the spacecraft trajectory are nearly the same, we can approximate the fluctuations $B'(r)$ by the increment of the field component $B_\Theta(r)$ between the measurements at two successive points r and r' at the spacecraft trajectory. The dipole part cancels out (high spatial resolution), and the increment $B'(r) = B_\Theta(r) - B_\Theta(r')$ represents an upper bound of the fluctuation. We estimate the error of calculating B' in this way to be less than 10%. The value $B'(r)$ is shown in Figure 5 for one typical spacecraft trajectory. The smooth solid line indicates the distance between the spacecraft and Jupiter. It ranges about between 9 and 16 Jupiter radii. Regions of two different types of fluctuations can be distinguished there.

[32] Nearly all regions show almost uncorrelated Gaussian noise corrupted by a beat frequency of 10.2 mHz due to the rotation of the spacecraft (about 51.8 mHz) and the sampling rate (41.7 mHz). The resulting period is clearly seen in the autocorrelation function $C(\mathbf{r}, \mathbf{r}') \approx \sigma_{B'}\,\delta(\mathbf{r} - \mathbf{r}')$ (Figure 6, bottom). This type of noise has been found almost everywhere in the inner regions of the Galileo orbits under consideration, i.e. $r \in (9\ldots 20)\ R_J$, except for the regions near the perijove of orbits under consideration.

[33] Around the closest approach of the Galileo spacecraft with Jupiter, the amplitudes of the fluctuations $\sigma_{B'}/B_0$ increase considerably and the statistical properties of the noise change. Although the estimated skewness $\gamma_{B'}$ (one characteristic feature) does not deviate strongly from zero, these high-amplitude fluctuations of the dipole strength deviate from a Gaussian distribution as shown in Figure 6. The distribution there seems to be composed of two Gaussian distributions. Additional effects are obviously at work in this inner Jovian system. On the other hand, compared to the time periods (or regions) when Gaussian fluctuations have been found, this non-Gaussian behavior is only of short duration. Thus in this study we exclude these fluctuations from consideration and leave them for future investigations. It does not mean, of course, that these stronger fluctuations do not influence the dynamics of the dust motes. It means that our findings have to be taken as a conservative treatment, i.e., we present what one has to expect at least from the influence of noise on the dust dynamics.

[34] The results for the other five spacecraft trajectories are very similar to those presented in Figures 5 and 6. Altogether, the low-amplitude uncorrelated Gaussian noise, found for most regions between 9 and 16 Jupiter

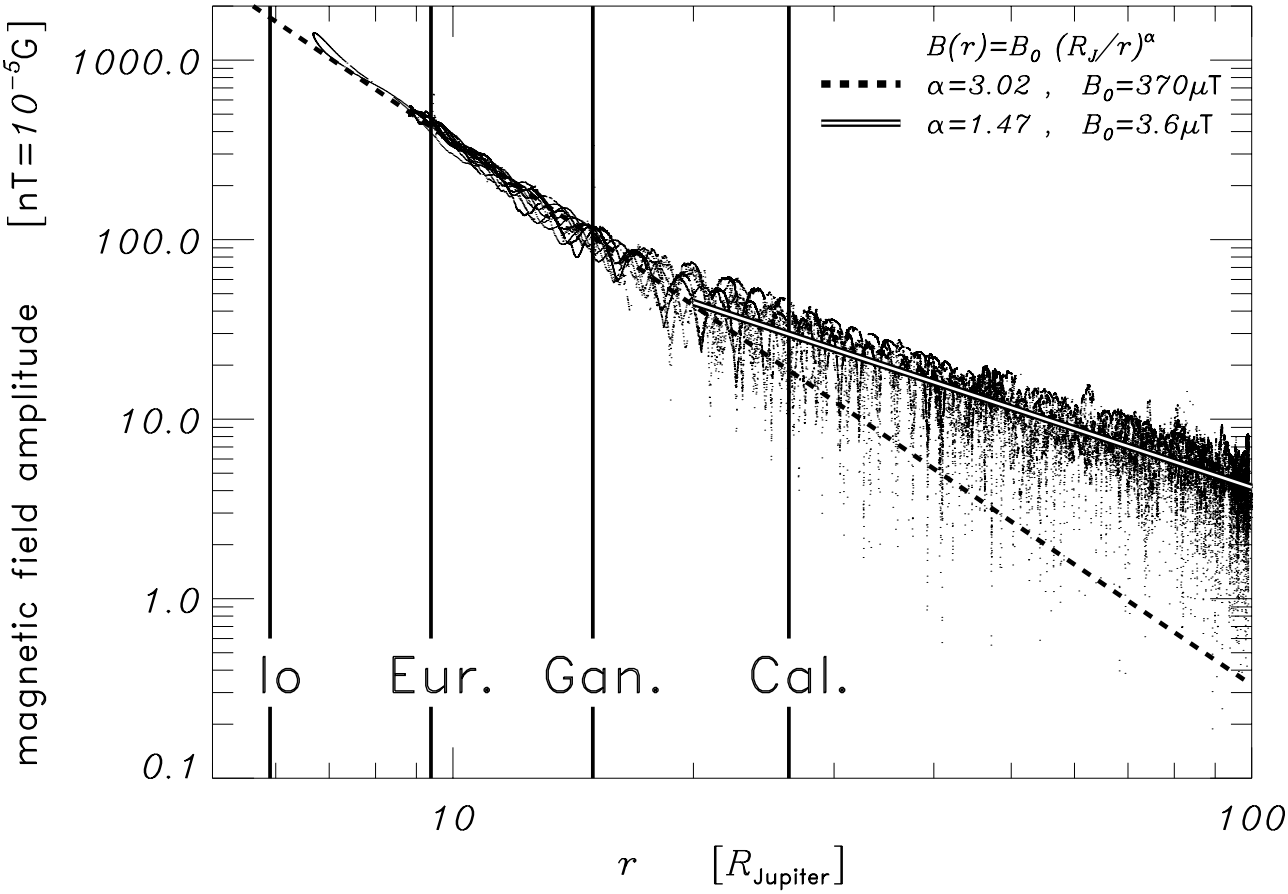

Figure 4. Log-log plot of the magnetic field versus the radial distance from Jupiter.

radii, justifies the assumptions of our analytical and numerical approaches in characterizing the influences of noise (section 2).

4. Conclusions

[35] In this paper we have studied the influence of a fluctuating magnetic field on the dynamics of charged circumplanetary dust. Specifically, we have considered micron-sized dust grains lost by Galilean satellites of Jupiter. These grains form a tenuous dust ring around the orbits of the Galileans, recently found in the dust detector data of the Galileo spacecraft [*Krivov et al.*, 2002]. The fluctuating magnetic field of Jupiter, characterized by a Gaussian white noise, causes in the first approximation an additive stochastic force. This problem has been treated with theoretical (analytical and numerical) methods, and the assumptions about statistical properties of noise have been checked with an analysis of the magnetometer data of the Galileo spacecraft.

[36] In this approximation (additive white noise) we have found a normal diffusion in the space of orbital parameters with superimposed undulations. According to our analytical study, the mean quadratic fluctuations of an orbital element x (eccentricity or inclination) obey the relation $\langle \Delta x^2 \rangle = D\,[t \pm \sin 2nt/(2n)]$, with the diffusion coefficient $D = \pi(|\Delta n|/n^2)\,\omega_G^2\,(B_s)$, where ω_G, B_s, n and $|\Delta n|$ are the gyrofrequency, autocorrelation of the magnetic field fluctuations, the Kepler frequency and the synodic forcing frequency, respectively.

[37] These analytical results have been confirmed by direct numerical simulations. We found that micron-sized grains from Europa, charged to +5 V, in about 100 years develop orbital eccentricities and inclinations up to 0.1 and 5°, respectively, provided that the fluctuations of the magnetic field have statistical properties described above. This is comparable to the perturbations imposed on the same grains by the deterministic part of the Lorentz force [*Krivov et al.*, 2002].

[38] In order to check whether the underlying assumptions of the stochastic model hold true, we have analyzed the magnetometer data obtained by the Galileo spacecraft during six selected orbits around Jupiter in 1997–2000. We have been interested mainly in the inner part of these orbits, at distances from ≈9 to 20 R_J (R_J is the Jupiter radius). We have found that the fluctuations of the magnetic field are Gaussian and white, except for a relatively narrow distance range around the perijoves where the fluctuations are much stronger obeying a bimodal/non-Gaussian distribution. This justifies the assumptions of the theoretical model and consequently, lends support to the theoretical prediction of a few percent diffusive changes of the inclinations and eccentricities for micrometer-sized particles. However, this has to be considered as a conservative estimate. The reasons are neglect of the strong non-Gaussian fluctuations in the innermost region, the

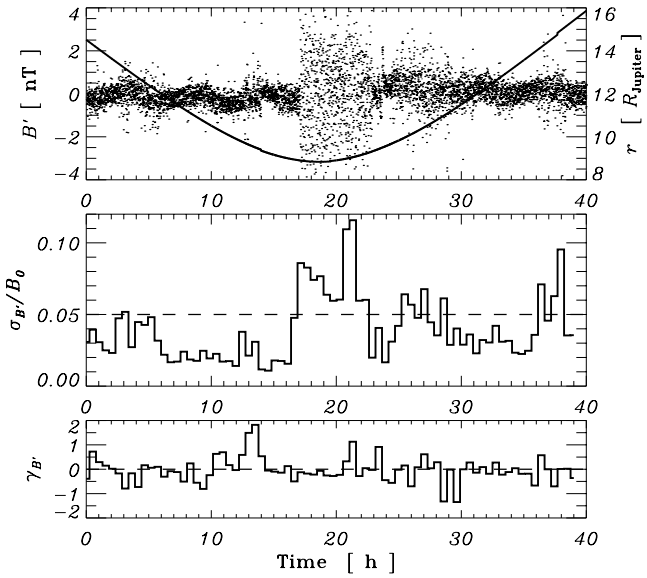

Figure 5. (top) The dots represent the fluctuating part of the magnetic field (dipole subtracted) versus time along the spacecraft trajectory on 28 March 1998. The solid line shows the distance to Jupiter. At the minimum distance of about 9 Jupiter radii the fluctuations increase up strongly. (middle) The estimated relative standard deviation (standard deviation divided by the average) of the fluctuation part of the magnetic field versus time. The dashed line shows the 5% level of the magnetic field fluctuations with respect to the dipole field strength. (bottom) The estimated skewness of the fluctuation part of the magnetic field versus time. The skewness is the dimensionless third moment (scaled with the standard deviation) of a data set.

assumption of small values for e and i, and accordingly, using the additive noise approximation.

[39] Regarding the effect of fluctuations on the dynamics of dust particles in circumplanetary environment, a strong mass/size-dependence must be mentioned. Assuming that the dust particles charge in quasi-equilibrium fashion to the same potential (+5 V in Jupiter's vicinity, see *Horányi* [1996]), the diffusion constant has a strong size dependence $D \propto r_p^{-4}$ (r_p is the radius of a spherical dust grain). This means that while micron-sized dust is already affected by stochasticity significantly, the dynamics of submicron motes are dominated by stochastic fluctuations. Related to this, the influence of multiplicative noise (colored noise) becomes quickly important for the dust dynamics. Furthermore, the influence of the stochastic fluctuations may be amplified by other effects, such as time variation of the charges (varying Lorentz force) or chaotic rotation of irregular-shaped grains (radiation pressure force).

[40] The role of these effects, most notably the influence of multiplicative noise, is an important issue for future analytical studies. It would also be extremely interesting to compare future theoretical predictions for submicrometer-sized dust grains with the Galileo dust detector data. Galileo did detect impacts of small grains, down to several tenths of a micron in radius, in the region of the Galilean satellites [*Thiessenhusen et al.*, 2000; *Krivov et al.*, 2002]. A difficulty, however, is that nearly all impacts of grains in this size regime occurred in the lowest amplitude range of the dust detector [*Grün et al.*, 1995; *Krüger et al.*, 1999], which is dominated by Jovian stream particles [e.g., *Grün et al.*, 1998]. No method has been found so far to identify and exclude this "contamination" from the data set (H. Krüger, personal communication, 2002).

[41] To summarize, in this paper we have demonstrated theoretically the performance and the aptitude of stochastic methods to assess the influence of fluctuations of the magnetic field on the dynamics of micrometer-sized grains in orbit around Jupiter. The theoretical results along with our analyses of the Galileo magnetometer data have shown that for these particles ($\approx$1 μm) the stochastic perturbations are comparable in strength to the deterministic ones. For submicrometer-sized particles much stronger effects have

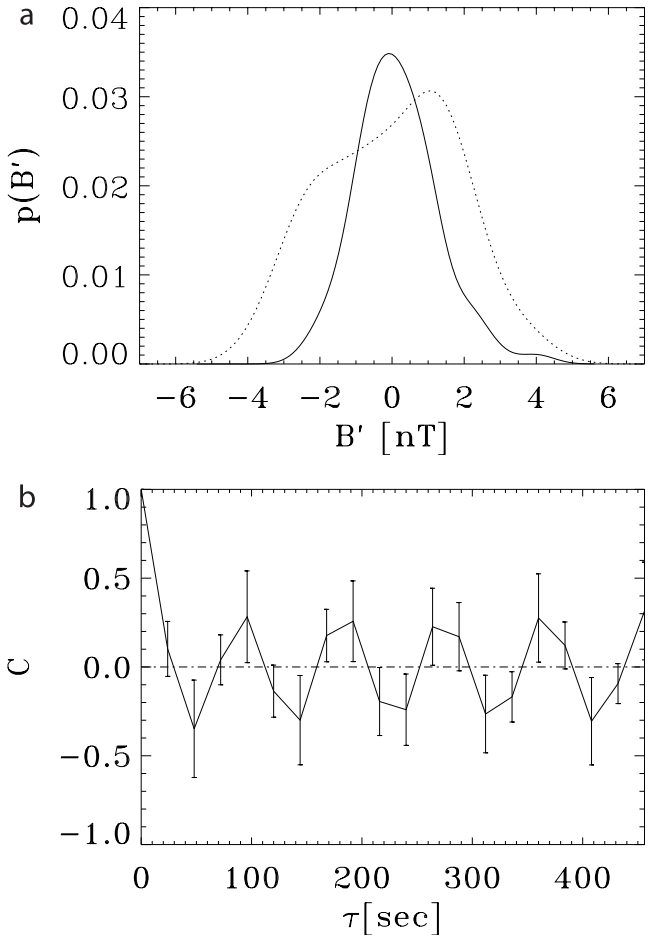

Figure 6. (top) Estimated probability density of the fluctuating part of the magnetic field far from the perijoves of Galileo (solid line) and close to the perijoves (dashed line; see also middle part of Figure 5). The Gaussian character of the fluctuations is modulated by an additional bump in the distribution. (bottom) The autocorrelation function of the fluctuating component shown in Figure 5. The beating period due to rotation of the spacecraft and the sampling rate is clearly seen. There is no significant correlation in the data beside this beat phenomenon. To estimate the error bars of the autocorrelation function we used 76 non-overlapping samples of 78 data points each along the spacecraft trajectory.

been predicted, which requires an extension of the theory to multiplicative-colored noise as perturbations.

[42] **Acknowledgments.** We wish to thank Margaret Kivelson and the magnetometer team of the Galileo project for providing us with the magnetic field data. Useful discussions with Guy Consolmagno, Larry Esposito, Eberhard Grün, Sascha Kempf, and Harald Krüger are very much appreciated. This work was funded by Deutsches Zentrum für Luft- und Raumfahrt (DLR), project 50 OH 0003, and by Deutsche Forschungsgemeinschaft (DFG), grant Sp 384/12-1.

References

Burns, J. A., M. R. Showalter, and G. E. Morfill, The ethereal rings of Jupiter and Saturn, in *Planetary Rings*, edited by R. Greenberg and A. Brahic, pp. 200–272, Univ. of Arizona Press, Tucson, 1984.

Burns, J. A., M. R. Showalter, D. P. Hamilton, P. D. Nicholson, I. de Pater, M. E. Ockert-Bell, and P. C. Thomas, The formation of Jupiter's faint rings, *Science*, *284*, 1146–1150, 1999.

Consolmagno, G., Lorentz scattering of interplanetary dust, *Icarus*, *38*, 398–410, 1979.

Consolmagno, G., Influence of interplanetary magnetic field on cometary and primaordial dust orbits: Applications of lorentz scattering, *Icarus*, *43*, 203–214, 1980.

Danby, J. M. A., *Fundamentals of Celestial Mechanics*, *2nd ed.*, Willmann-Bell, Richmond, VA., 1988.

Everhart, E., Implicit single-sequence methods for integrating orbits, *Celest. Mech. Dynam. Astron.*, *10*, 35–55, 1974.

Everhart, E., An efficient integrator that uses Gauss-Radau spacing, in *Dynamics of Comets: Their Origin and Evolution*, edited by A. Carusi and G. B. Valsecchi, pp. 185–202, Dordrecht, Reidel, 1985.

Gardiner, C. W., *Handbook of Stochastic Methods*, Springer, Berlin, Heidelberg, 1983.

Grün, E., M. Baguhl, H. Fechtig, D. P. Hamilton, J. Kissel, D. Linkert, G. Linkert, and R. Riemann, Reduction of Galileo and Ulysses dust data, *Planet. Space Sci.*, *43*, 941–951, 1995.

Grün, E., H. Krüger, A. Graps, D. P. Hamilton, A. Heck, G. Linkert, H. A. Zook, S. Dermott, H. Fechtig, B. A. Gustafson, M. S. Hanner, M. Horányi, J. Kissel, B.-A. Lindblad, D. Linkert, I. Mann, J. A. M. McDonnell, G. E. Morfill, C. Polanskey, G. Schwehm, and R. Srama, Galileo observes electromagnetically coupled dust in the jovian magnetosphere, *J. Geophys. Res.*, *103*, 20,011–20,022, 1998.

Hänggi, P., and H. Thomas, Stochastic processes, *Phys. Rep*, *88*, 251–342, 1982.

Horányi, M., Charged dust dynamics in the Solar System, *Annu. Rev. Astron. Astrophys.*, *34*, 383–418, 1996.

Horányi, M., and T. E. Cravens, The structure and dynamics of Jupiter's ring, *Nature*, *381*, 293–295, 1996.

Horányi, M., J. A. Burns, and D. P. Hamilton, The dynamics of Saturn's E ring particles, *Icarus*, *97*, 248–259, 1992.

Kivelson, M. G., K. K. Khurana, J. D. Means, C. T. Russell, and R. C. Snare, The Galileo magnetic field investigation, *Space Sci. Rev.*, *60*, 357–383, 1992.

Kivelson, M. G., J. Warnecke, L. Bennett, S. Joy, K. K. Khurana, J. A. Linker, C. T. Russell, R. J. Walker, and C. Polanskey, Ganymede's magnetosphere: Magnetometer overview, *J. Geophys. Res.*, *103*, 19,963–19,972, 1998.

Klačka, J., Interplanetary dust particles and solar radiation, *Earth, Moon and Planets*, *64*, 125–132, 1994.

Krivov, A. V., H. Krüger, E. Grün, K. Thiessenhusen, and D. P. Hamilton, A tenuous dust ring of Jupiter formed by escaping ejecta from the Galilean satellites, *J. Geophys. Res.*, *107*, doi:10.1029/2000JE001434, 2002.

Krüger, H., et al., Three years of Galileo dust data: II, 1993 to 1995, *Planet. Space Sci.*, *47*, 85–106, 1999.

Mannella, R., A gentle introduction to the integration of stochastic differential equations, in *Stochastic Processes in Physics, Chemistry, and Biology*, edited by J. A. Freund and T. Pöschel, pp. 353–364, Dordrecht, Springer, 2000.

Mannella, R., and V. Palleschi, Fast and precise algorithm for computer simulation of stochastic differential equations, *Phys. Rev. A*, *40*, 8031–8033, 1989.

Morfill, G. E., E. Grün, and T. V. Johnson, Dust in Jupiter's magnetosphere: Physical processes, *Planetary and Space Science*, *28*, 1087–1100, 1980a.

Morfill, G. E., E. Grün, and T. V. Johnson, Dust in Jupiter's magnetosphere: Effect on magnetospheric Electrons and Ions, *Planetary and Space Science*, *28*, 1115–1123, 1980b.

Spahn, F., K.-U. Thiessenhusen, J. Colwell, R. Srama, and E. Grün, Dynamics of dust ejected from Enceladus: Application to the Cassini dust detector, *J. Geophys. Res.*, *104*, 24,111–24,120, 1999.

Thiessenhusen, K.-U., H. Krüger, F. Spahn, and E. Grün, Large dust grains around Jupiter—The observations of the Galileo dust detector, *Icarus*, *144*, 89–98, 2000.

A. V. Krivov, J. Kurths, U. Schwarz, F. Spahn, and M. Sremčević, Department of Nonlinear Dynamics, Institute of Physics, University of Potsdam, Postfach 601553, 14469, Potsdam, Germany. (krivov@agnld.uni-potsdam.de; jkurths@agnld.uni-potsdam.de; shw@agnld.uni-potsdam.de; frank@agnld.uni-potsdam.de; msremac@agnld.uni-potsdam.de)